

Electrical-transport properties of $\text{Fe}_3\text{O}_4/\text{NiO}$ superlattices

G. Chern, S. D. Berry, D. M. Lind, H. Mathias, and L. R. Testardi

Department of Physics and the Center for Materials Research and Technology (MARTECH),

Florida State University, Tallahassee, Florida 32306

(Received 9 April 1991; revised manuscript received 11 September 1991)

We have utilized molecular-beam-epitaxy techniques in an electron-cyclotron-resonance oxygen plasma to synthesize thin films of NiO, Fe_3O_4 (magnetite), and modulated structures of these compounds with repeat structures of $(17 \text{ \AA})/(17 \text{ \AA})$, $(34 \text{ \AA})/(34 \text{ \AA})$, and $(68 \text{ \AA})/(68 \text{ \AA})$. The current-voltage (I - V) relation has been measured for current parallel and perpendicular to the planes, for temperature from 5 to 300 K, and with electric fields E up to 10^5 V/cm. All samples show strong nonlinear effects in the I - V behavior with I/V proportional to $\exp(cE^{1/2})$. For NiO and Fe_3O_4 , c is approximately proportional to $1/T$ below 100 K, as expected for Poole-Frenkel conduction and, on the basis of this interpretation, yields dielectric constants of 4.1 and 10.1, respectively. A nonmonotonic temperature dependence of c occurs for the modulated structures with a minimum in the field dependence occurring at 40 K. The low-field conductivities found for pure NiO and Fe_3O_4 films are similar to those reported for the bulk at the higher temperatures, with Fe_3O_4 films also showing the Verwey transition at 120 K. In the $(34 \text{ \AA})/(34 \text{ \AA})$ modulated structure, the electrical conductivity and its temperature dependence are consistent with pure Fe_3O_4 in the low-temperature phase, but the Verwey transition upon warming to the high-conductivity phase does not occur at any $T < 300$ K, suggesting that low-dimensionality effects may alter the transition. The $(34 \text{ \AA})/(34 \text{ \AA})$ modulated structure also shows a low- E -field conductivity anisotropy of 10^6 or greater, which is comparable to the largest known values for any material. We give arguments why modulated structures may modify the electrical-transport properties of material containing Bohr-like impurity states and show that $\text{Fe}_3\text{O}_4/\text{NiO}$ may be such a case. We conclude that a modulated and E -field-variable conductivity of many orders of magnitude can be achieved in the modulated structures on a length scale of tens of angstroms, which suggests the possibility of voltage-controlled superlattice phenomena.

I. INTRODUCTION

The insulating and metallic states of transition-metal oxides have been often studied due to their rich variety of electrical properties.^{1,2} The electrical conductivities of these materials may differ by many orders of magnitude, even though they have similar structures. A well-known problem for these materials, however, is that the preparation of high-quality, i.e., low-defect, stoichiometric single crystals is very difficult.^{1,3} As a result of this, many early studies did not emphasize the intrinsic properties of these materials. The research on the syntheses and characterizations of the thin films and multilayered structures of oxides is still in an early stage. In these early works, Bando and collaborators, for instance, successfully fabricated NiO, CoO, Fe_3O_4 thin films and superlattices on different substrates.⁴⁻¹¹ Other oxides such as MgO and titanates were also grown and studied by others.^{12,13} Recently, significant research attention has been focused on electron transport in oxides, after high-temperature superconductivity was found in layered perovskite oxides.

We have recently fabricated a series of iron oxide and nickel oxide thin films and superlattices of these two materials by an oxygen-plasma-assisted molecular-beam epitaxy (MBE). The aim of these studies is to understand the structure, surface morphology, magnetic hysteresis, and electrical transport properties through reflection

high-energy electron diffraction (RHEED), x-ray diffraction (XRD), scanning electron microscopy (SEM), superconducting quantum interference device magnetometry, and conductivity measurements. The results of these studies showed that these thin films are likely to be stoichiometric single crystals. The electric and magnetic characteristics of the pure thin films are similar to those of the bulk. The superlattice films showed interesting magnetic properties which are very sensitive to the superlattice wavelength. The electrical conductivity of these superlattices showed a substantial anisotropy: the current flow parallel to the films is orders of magnitude larger than current flow perpendicular to the films. In this paper we report experimental results on the electric conductivity of these materials from room temperature to liquid-helium temperature. Structural and magnetic studies of these films are reported elsewhere.^{14,15}

Although both NiO and Fe_3O_4 have been heavily studied for the last sixty years, the basic conduction mechanism in these materials is still an open issue. NiO is an antiferromagnetic insulator, with a conductivity of about $10^{-10} (\Omega \text{ cm})^{-1}$ at room temperature, which varies as a function of temperature as a typical semiconductor. It does not form a metallic state above the Néel temperature; therefore, it is generally accepted that the electrons are highly correlated and a Hubbard-type model has been suggested to interpret the insulating state.^{1,16}

Fe_3O_4 has a metal-insulator (Verwey) transition at around $T_v = 120$ K. Below this temperature it is an insulator with a gap of about 70 meV at $T \approx 50$ K. Around the transition temperature, the conductivity increases by a factor of 100 and becomes very weakly temperature dependent above the transition temperature. Mott suggested that at low temperature a Wigner-type crystallization formed and above the T_v the disorder state is favored. However, the basic mechanism for the sudden increase of the conductivity at the transition has still not been completely resolved.^{3,17}

Superlattices are made by combining two different materials into a layered structure with an artificial periodicity along the perpendicular, growth direction. The ultimate goal of our studies is to develop a fabrication technique for transition-metal oxide superlattices. Our particular choice of this system is based on the good lattice match between the parent materials and the MgO substrate which helps the stabilization of the superlattice structures. However, this system provides an interesting opportunity for a study of the conductivity for the following reasons: (1) Although both materials are metal oxides, the conductivities differ by about 10 orders of magnitude; hence effect on the conductivity due to the superlattice structure should be seen rather easily. (2) The basic conduction mechanism of the oxides is due to electron hopping and the small mean free path of the electrons implies that electrical properties can be maintained within a very small length scale. (3) It provides an opportunity to see whether the Verwey transition is affected by the modulated structures. (4) By studying the conductivity of the superlattice with different superlattice wavelengths, we hope that we will learn both the applications and basic transport mechanisms of these interesting transition-metal oxides.

We briefly describe the growth process and the conductivity measurement in Sec. II. Then we report the experimental results in Sec. III. Finally, Sec. IV contains discussions and conclusions. A preliminary account of the electrical anisotropy of the superlattice samples has been published elsewhere.¹⁸

II. EXPERIMENTAL

Since a full description of the MBE system and the growth conditions are given elsewhere,¹⁴ we only briefly

mention some details, as follows. High-purity Ni and Fe were used in two separated *e*-beam sources. The substrate was held by a manipulator vertically facing down. A quartz-crystal thickness monitor was mounted next to the substrate and was used to monitor the deposition rate. Two highly sensitive pneumatically driven shutters were also controlled by the thickness monitor so that a superlattice thin film can be formed by alternately shuttering the two sources. Typical deposition flux rates were set around 2–3 Å/sec. A resistive heating state was used to maintain the substrate temperature during growth at 250 C. Oxygen was introduced through an electron cyclotron resonance plasma source. Typical base pressure in the chamber is 1×10^{-9} Torr. The pressure during growth with oxygen is 3×10^{-6} Torr, with the (residual-gas-analyzer—measured) background partial pressure other than oxygen below 1×10^{-10} Torr. A total of nine samples was used in this study. These samples were grown on substrates with and without conducting layers so that the conductivity could be measured either parallel to the layers or perpendicular to the layers (hereafter called parallel and perpendicular configurations, respectively). The samples for the parallel configuration were grown on polished MgO (001) surfaces; high-quality pure and superlattice thin films were determined by the SEM and XRD studies. The samples for the perpendicular configuration were made on 500–600-Å Ni base layer coated on Mica *in situ*, and the films usually were polycrystalline. However, they have preferred (111) orientation, and modulated structures which were also confirmed by the XRD. The structural coherency and the sharp interfaces of these films were revealed by *in situ* RHEED and *ex situ* XRD. RHEED patterns showed the evolution of Fe_3O_4 to NiO within 1 monolayer, and NiO to Fe_3O_4 within 4–5 monolayers. XRD results typically showed five or more side bands on each side of the main peak for the parallel configuration samples, which supports the idea of the structural coherency and sharp interfaces. XRD rocking curve measurements were also carried out. Typical rocking linewidth is (full width at half maximum) 0.095° (instrumental resolution $\approx 0.05^\circ$) which corresponds to a variation in lattice spacing of 0.00021 Å or 0.10% of the interlayer spacing. XRD results showed small ($< 10\%$) deviations of the modulation wavelength from those set by the thickness monitor and energy dispersive x-ray

TABLE I. Description of samples and measurements.

Sample	Substrate	Thickness (Å)	Measurement
Fe_3O_4	MgO (001)	10 000	in plane
NiO	MgO (001)	10 000	in plane
(17 Å)/(17 Å) ^a	MgO (001)	10 000	in plane
(34 Å)/(34 Å) ^a	MgO (001)	10 000	in plane
Fe_3O_4	Ni-coated Mica	5 000	cross plane
NiO	Ni-coated Mica	5 000	cross plane
(17 Å)/(17 Å) ^a	Ni-coated Mica	3 570	cross plane
(34 Å)/(34 Å) ^a	Ni-coated Mica	5 030	cross plane
(68 Å)/(68 Å) ^a	Ni-coated Mica	8 160	cross plane

^aThese are nominal related compositions. Energy dispersive x-ray analysis measurements show variations of $< 10\%$ from these values.

analysis showed deviation $<10\%$ from the assumed equal thickness structures (50% NiO and 50% Fe_3O_4). The superlattice samples have different superlattice periodicities along the perpendicular direction and we use $(n \text{ \AA})/(n \text{ \AA})$ to represent a sample which has nominally $n \text{ \AA}$ of Fe_3O_4 and NiO each. The nominal values are used below. The total thickness of these samples varies from 0.35 to $1 \mu\text{m}$ and is also listed in Table I. The conductivity measurements were accomplished using two-probe silver-paste contacts as a function of the temperature from 5–300 K. Due to the strong nonlinear dependence of the conductivity on the electric field, the perpendicular data were obtained by measuring the current as a function of a triangular-shaped voltage ramp which is generated from a synthesizer with the voltage spanning -10 – 10 V . These materials have high resistivity at low temperature so that contact resistance (\approx a few Ω) can be neglected.

III. RESULTS

A. Current-voltage nonlinear effect

Some representative current-voltage (I - V) curves of these measurements are presented in Fig. 1. A very strong nonlinear behavior can be seen. Notice that the electrical fields for these measurements can be as high as 10^5 V/cm because the sample thicknesses are $<1 \mu\text{m}$. This strong nonlinearity in I - V profiles was seen on all of the perpendicular configuration samples. Generally it becomes more pronounced as the temperature is lowered. These I - V curves are largely symmetrical with bias voltage; small deviations are due to temperature fluctuations. No nonlinear effects can be seen for the parallel configuration samples probably because the electric fields are much lower.

B. Square root of electric-field dependence

Different analytical functional forms have been tested to fit these non-Ohmic data. An exponential of the

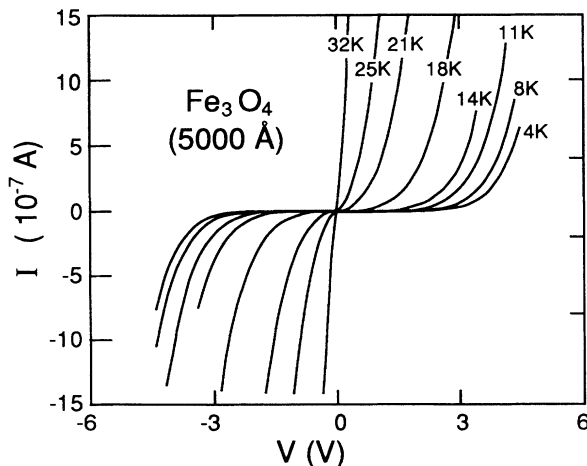


FIG. 1. Representative series of I - V curves of the 5000-\AA Fe_3O_4 film measured at the temperatures between 4 and 32 K. Similar nonlinear I - V behaviors were observed for all of the perpendicular configuration samples.

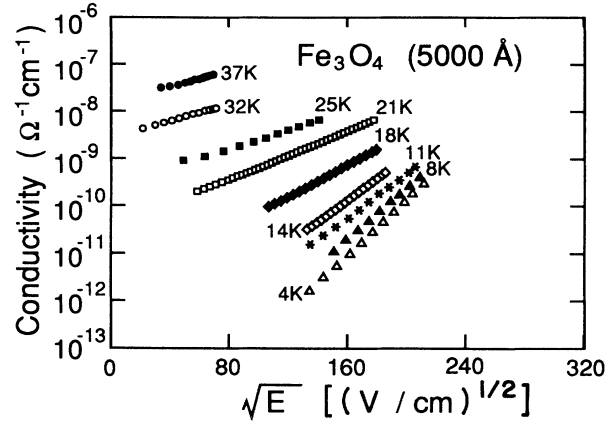


FIG. 2. The perpendicular conductivity of a Fe_3O_4 film as a function of the square root of electric field on a semilog plot.

square root of the electric-field dependence gives the best fit for all of the data. These plots are shown in Figs. 2–6 for Fe_3O_4 , NiO, and the superlattice samples. The lower field data were typically noisier, probably due to the very low current and conductance. Those lower field data are truncated from Figs. 2–6. Notice that these nonlinear effects are material dependent so that some measurements can reach lower temperatures before they reach the equipment limitation.

Electric-field-dependent non-Ohmic behaviors have been observed in some semiconductors, transition-metal oxide glasses, and other materials.¹⁹ The origins of these non-Ohmic conductivities can arise from electrode, heating, and bulk effects. For our samples, the first two possibilities are unlikely because (1) of the low adiabatic heating which we have calculated, and (2) all the I - V curves are well retraced without showing any hysteresis. The square root of electric-field dependence is believed to be a result of the Poole-Frenkel effect which has been observed in many semiconductor materials. The ionization energy W is modified by the electric field E , so that the conductivity for intrinsic (or noncompensated extrinsic) materials has the following (cgs) form:

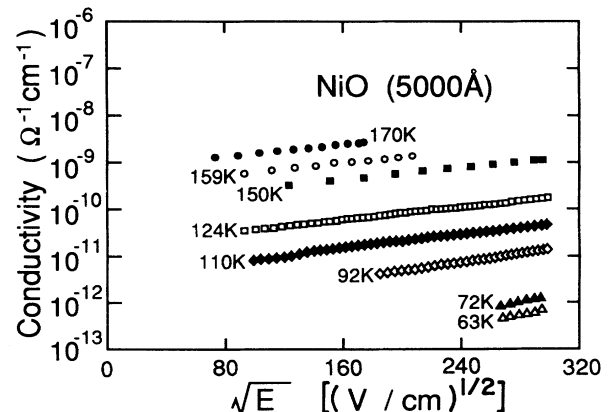


FIG. 3. The perpendicular conductivity of a NiO film as a function of the square root of electric field on a semilog plot.

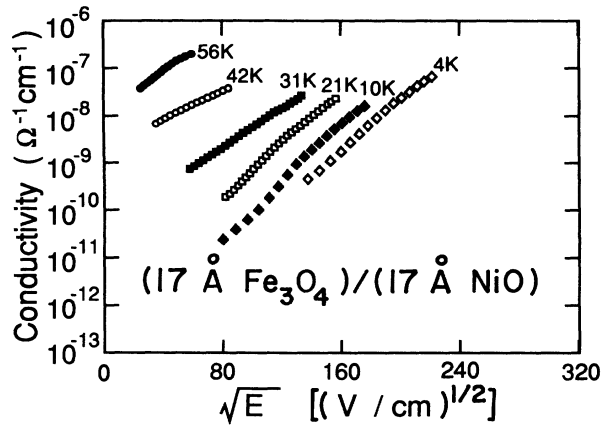


FIG. 4. The perpendicular conductivity of a (17 Å)/(17 Å) film as a function of the square root of electric field on a semilog plot.

$$\sigma(T) = \sigma_0(T) \exp\left[-\frac{1}{2}(W - \beta_i E^{1/2})/kT\right], \quad (1)$$

where $\sigma_0(T)$ is a weakly temperature-dependent prefactor, k is the Boltzmann constant, $\beta_i = 2e^{3/2}/K^{1/2}$, and K is the dielectric constant. More discussions about field-dependent hopping and the Poole-Frenkel effect can be found in, for example, Ref. 20.

The slopes of the data in Figs. 2–6 give the characteristic field constants of the samples and are related to the dielectric constant of the materials if the Poole-Frenkel mechanism is applied. In Fig. 7(a) we plot the slopes as a function of $1/T$ for Fe_3O_4 and NiO. For Fe_3O_4 , the best fit for the linear part ($T > 10$ K) gives dielectric constant $K = 10.1$. At very low temperatures ($T < 10$ K) it becomes very weakly temperature-dependent. A similar behavior has also been seen, for instance, in amorphous carbon films,²¹ and Mott later suggested that this can be explained by a high-field variable-range-hopping mechanism.²⁰ Due to the high resistivity, experimental constraints only allowed the NiO data to be limited at somewhat higher temperature and they roughly fit to a straight line with $K = 4.1$.²² As can be seen in

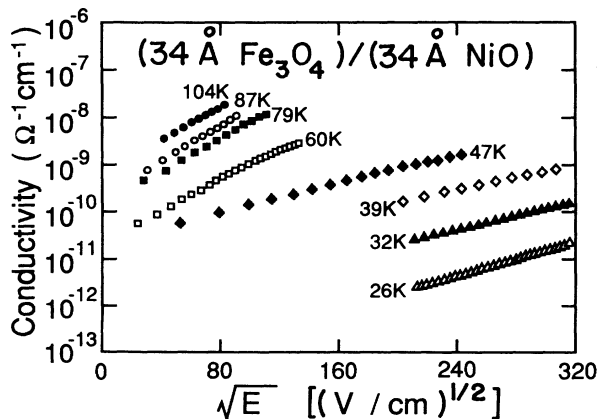


FIG. 5. The perpendicular conductivity of a (34 Å)/(34 Å) film as a function of the square root of electric field on a semilog plot.

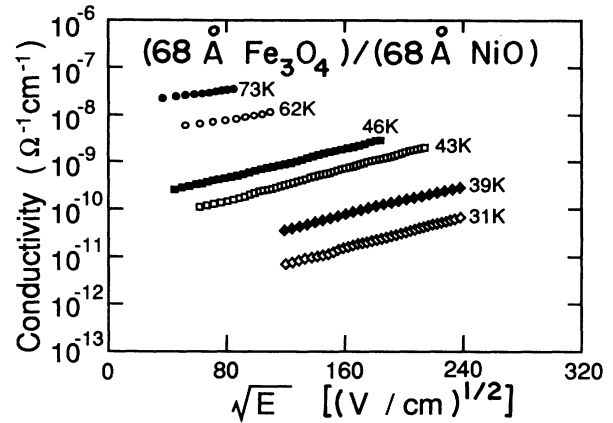


FIG. 6. The perpendicular conductivity of a (68 Å)/(68 Å) film as a function of the square root of electric field on a semilog plot.

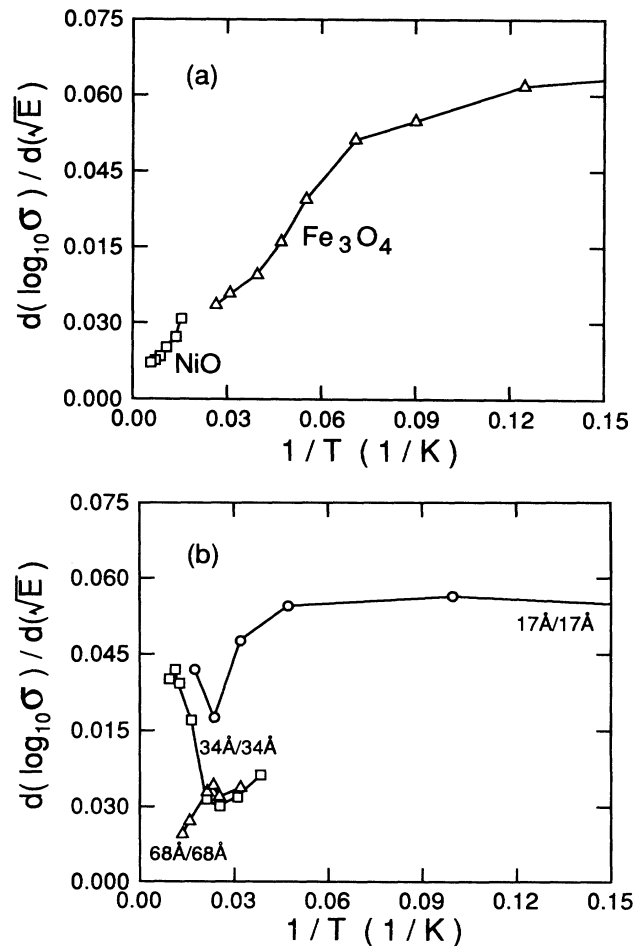


FIG. 7. (a) Plots of $d(\log_{10}\sigma)/d(E^{1/2})$ as a function of the reciprocal temperature for Fe_3O_4 and NiO. The linear parts give rough estimates for the dielectric constants 10.1 and 4.1 for Fe_3O_4 and NiO, respectively. (b) Plots of $d(\log_{10}\sigma)/d(E^{1/2})$ as a function of the reciprocal temperature for superlattices. Both (17 Å)/(17 Å) and (34 Å)/(34 Å) samples show anomalous minima around 40 K and the (68 Å)/(68 Å) sample also shows a weak kink around that temperature. The y-axis units for Figs. 7(a) and 7(b) are $[(\text{V}/\text{cm})^{-1/2}]$.

Fig. 7(b), unlike the pure materials, the superlattice samples completely lose the inverse temperature characteristics and an anomalous minimum occurs around 40 K for the (17 Å)/(17 Å) and (34 Å)/(34 Å) samples. A similar minimum was also seen on the (68 Å)/(68 Å) sample, although somewhat weaker.

C. Low electrical field conductivity

The low-field perpendicular conductivities (σ_{\perp}) for these samples were obtained by extrapolating the data from the square root of E -dependent plots to $E=0$. In Fig. 8 we show these results as a function of the reciprocal temperature. Most of these curves showed typical characteristics of semiconductors. The conductivities of both Fe_3O_4 and NiO agree with the bulk values reasonably well at around 50 and 300 K, respectively. The conductivities of the superlattices generally fall in between the pure materials in the same temperature region. The (68 Å)/(68 Å) sample data overlap the (34 Å)/(34 Å) sample data around 30 K with their conductivities being between those of Fe_3O_4 and NiO. However, the conductivity of the (17 Å)/(17 Å) samples tends to reach the Fe_3O_4 value or even slightly higher at temperatures below 20 K.

For the parallel configuration samples, since the conductivity (σ_{\parallel}) was Ohmic, the σ_{\parallel} was simply measured continuously as a function of the temperature. These data are also plotted in the top part of Fig. 8 so that a comparison can be made between these two configurations. Some important observations can be pointed out: (1) The Verwey transition around 120 K is clearly seen for the Fe_3O_4 sample. (2) The conductivity of the (34 Å)/(34 Å) is almost the same as the Fe_3O_4 sample below 120 K but with no sign of the Verwey transition around 120 K.

The parallel conductivity of NiO is too low for us to measure. Only an upper bound about $10^{-7} (\Omega \text{ cm})^{-1}$ at room temperature was obtained.

The most instructive results made in this study are in

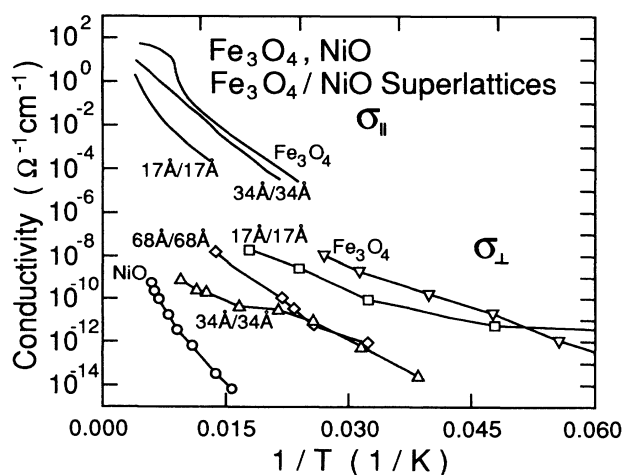


FIG. 8. Perpendicular and parallel conductivities (σ_{\parallel} and σ_{\perp}) of Fe_3O_4 , NiO, and $\text{Fe}_3\text{O}_4/\text{NiO}$ superlattices as a function of the reciprocal of the temperature. A large anisotropy, $\sigma_{\parallel}/\sigma_{\perp} = 10^6$, is found for the (34 Å)/(34 Å) modulated structures.

the comparison of the conductivity along two different directions: (1) A substantial anisotropy, $\sigma_{\parallel}/\sigma_{\perp}$, is seen in the (34 Å)/(34 Å) and (17 Å)/(17 Å) samples reaching 10^6 and 10^2 , respectively. (2) The conductivity anisotropy of the Fe_3O_4 around 50 K also reaches a factor of 100. However, *in situ* RHEED has evidence that a thin NiO film was possibly formed on the Ni buffer layer and this may cause higher resistivity results on perpendicular Fe_3O_4 . More discussions of this effect are given later. (3) The parallel results typically cover higher temperature regions compared to the perpendicular ones, and overlaps between the two configurations are quite limited. This is due to the length-to-area ratio which is very different for these two configurations.

IV. DISCUSSIONS

A. Thin-film quality

Our Fe_3O_4 films have resistivities at 300 K within 30% of those reported for bulk materials,²³ show an onset of the Verwey (metal-to-insulator) transition T_v on cooling at ≈ 120 K similar to bulk values,²³ and exhibit drops in conductivity through the transition of $1\frac{1}{2}$ orders of magnitude compared to 2 orders for the bulk. Below T_v the film conductance falls with a temperature dependence $\exp(-E_g/kT)$ having, in the vicinity of 50 K, $E_g = 56$ meV compared to 70 meV in the bulk.

For NiO our measured conductivity at $T = 170$ K (the highest measurement T was $10^{-9} (\Omega \text{ cm})^{-1}$) compared to reported bulk values²⁴ which cover the range $10^{-6} - 10^{-12} (\Omega \text{ cm})^{-1}$ at this temperature and include the value $10^{-10} (\Omega \text{ cm})^{-1}$ for single-crystal NiO.

B. The effect of superlattice structure on nonlinear electrical conductivity

It is easy to show that for a field-dependent conductivity of the Poole-Frenkel type, previously given by Eq. (1), the transverse conductivity of an equal-thickness composite with $\sigma_h \gg \sigma_l$, is now given by

$$\sigma_{\perp}(T) \approx 2\sigma_{l0} \exp\left[(2^{1/2})\frac{1}{2}\beta E^{1/2}/kT\right], \quad (2)$$

where σ_{l0} is the temperature-dependent low-field conductivity of the lower conductivity component (NiO) and the additional $2^{1/2}$ factor in the field dependence arises from the fact that the field exists only over this latter component. Thus, for the modulated structure behaving as a composite material one expects the field dependence of the conductivity to resemble that of the NiO slab (which again may not be similar to pure NiO in behavior) except for a factor-of- $2^{1/2}$ increase in the field exponent. This is equivalent to shifting downward by a factor of $2^{1/2}$ all of the modulated structure data of Fig. 7(b). Note, however, that the observed field dependence of the modulated structure conductivity is larger than that of NiO, and is nonmonotonic in temperature. At $T > 50$ K a temperature dependence opposite to that of pure NiO is found for the (34 Å)/(34 Å) and (17 Å)/(17 Å) structures. Both field dependencies are about three times larger than that of NiO at above 50 K and decrease reaching minima

around 40 K. The $(68 \text{ \AA})/(68 \text{ \AA})$ structure shows much better agreement with NiO but still shows a weak kink at 40 K. Thus, the data show that the shorter-wavelength modulated structures undergo a transition near 40 K in the field dependencies of their electrical conductivities while no such behavior is found for the pure constituents in their bulk behavior. Since this anomaly does depend on the superlattice wavelength, it is speculated that the response of the thin-layer NiO to the electric field strongly depends on the layer thickness and the temperature.

One expected effect of modulated structures on the Poole-Frenkel effect would be the destruction of all Bohr orbits for the impurity states when the diameter of the first orbit, approximately given by $D_b \approx 1.06 \text{ K}/(m^*/m) \text{ \AA}$, where m^* and m are the effective mass and free electron mass, respectively, is greater than half the modulation wavelength. For many semiconductors this orbit size is $\approx 10\text{--}100 \text{ \AA}$. This orbital diameter covers the range of our modulated-structure half wavelengths for which we do find the Poole-Frenkel effect to be modified compared to the pure materials. Note that this argument sets a length scale for electrical conductivity which is possibly longer than the mean free path, and thus the more important one for electrical transport in a modulated structure. A further consequence is that the energy of this orbit, $E_b \approx 13.6(m^*/m)/K^2 \text{ eV}$, which is $\approx 10\text{--}50 \text{ meV}$ in typical semiconductors, could result in modified temperature dependencies below the corresponding temperature range 100–500 K where the orbits should be occupied. Using values between 4.1 (NiO) and 10.1 (Fe_3O_4) obtained in our pure films from the Poole-Frenkel effect would lead to $m^*/m \approx 0.1\text{--}0.4$ for total orbit destruction effects in the $(34 \text{ \AA})/(34 \text{ \AA})$ superlattice. This effective mass ratio is not physically unreasonable, but we know of no confirming evidence. Modulated structures may also provide range restrictions for hopping conduction processes, but we have not attempted numerical estimates.

C. The effect of superlattice structure on electrical anisotropy

A two-component equal-thickness-layered composite of materials having field-independent conductivities σ_h and σ_l , with $\sigma_h \gg \sigma_l$, will have approximate effective conductivities

$$\sigma_{\parallel} \approx \sigma_h/2, \quad (3)$$

$$\sigma_{\perp} \approx 2\sigma_l, \quad (4)$$

where σ_{\parallel} and σ_{\perp} correspond to cases of current flow parallel and perpendicular to the layer planes. Thus, the component conductivity ratio can be determined from the composite conductivity anisotropy

$$\sigma_{\parallel}/\sigma_{\perp} \approx \frac{1}{4}\sigma_h/\sigma_l. \quad (5)$$

In the limit of composition modulation wavelength $\lambda \rightarrow \infty$, one expects to obtain the bulk value ratio σ_h/σ_l . For small λ the ratio will differ from the bulk value partly due to the imperfection of the chemical and structural modulation (and thus be a measure of the degree of modulation), but also because of possible reduced dimen-

sionality effects as $\lambda \rightarrow 0$. Although Eqs. (3)–(5) are based on the approximation $\sigma_h/\sigma_l \gg 1$, which is certainly true for the Fe_3O_4 and NiO of our experiment, the measured conductivities σ_{\parallel} and σ_{\perp} are reliably obtained only if the corresponding conductivities for the two-current paths are such that the assumed one-dimensional current flow is nearly true. The length-to-area ratios for the \parallel and \perp cases in our experiments are such that the maximum anisotropy in σ_c which can be measured is $\approx 10^6$. We shall show that this limiting value is, indeed, found in our measurements for the modulated structures.

Figure 8 gives the temperature dependence of σ_{\parallel} and σ_{\perp} and shows the existence of remarkable anisotropy for structures with $(34 \text{ \AA})/(34 \text{ \AA})$ (and possibly smaller) modulation. The most unusual result is that the anisotropy $\sigma_{\parallel}/\sigma_{\perp}$ for the $(34 \text{ \AA})/(34 \text{ \AA})$ modulated structure for T between 50 and 100 K lies between 10^6 and 10^8 , among the largest of any known material and, indeed, at the upper limit of our experimental capability. This large anisotropy could suggest a possible state of simulated two-dimensional conduction of the Fe_3O_4 if the characteristic length for electrical transport in this compound were $\geq 34 \text{ \AA}$, but we do not know if such a length is appropriate.

The ability to maintain 6 or more orders of magnitude difference in the conductivity of NiO and Fe_3O_4 down to a length scale of 34 \AA , and perhaps 2 orders of magnitude at 17 \AA , attests to the degree of chemical modulation which can be obtained at such short wavelengths, and to the degree of locality of the electrical conduction, at least in the NiO. The spatially modulated electrical conductivity of 6 orders of magnitude for $(34 \text{ \AA})/(34 \text{ \AA})$, and possibly 2 orders of magnitude for the $(17 \text{ \AA})/(17 \text{ \AA})$ structure will, of course, be accompanied by a comparable spatial modulation of the electric field and its gradient along the modulation direction when a voltage is applied. This suggests the possibility of introducing a superlattice electric field, nonlinear in the applied voltage, which may lead to new phenomena.

It should be pointed out that for Fe_3O_4 the σ_{\perp} data which appear to lie 2 orders of magnitude below the σ_{\parallel} data may, in fact, be corrupted by a small amount of NiO which can form at the Ni base layer during the initial stages of the Fe_3O_4 layers. An examination of σ_{\parallel} data for the modulated structures shows that if $\approx 20 \text{ \AA}$ of NiO forms at that interface which is similar in conductivity to what occurs in a $(17 \text{ \AA})/(17 \text{ \AA})$ modulated structure, then that added resistance can dominate the measurement and reduce the measured conductance by 2 orders of magnitude. Such a layer cannot be discounted, and therefore the σ_{\perp} data for pure Fe_3O_4 may be treated as a lower limit. This argument does not apply, however, for the modulated structures or NiO.

D. The effect of superlattice structures on the Verwey transition

Equation (3) shows that the conductivity σ_{\parallel} for an equal-thickness-modulated structure of Fe_3O_4 and NiO will have a value of half that of the Fe_3O_4 layer of that

structure (which need not be bulklike). Figure 8 shows that for T below 110 K, σ_{\parallel} for the (34 Å)/(34 Å) film is approximately half that of the pure Fe_3O_4 film. From this result we see that the conductivity of the Fe_3O_4 layers in (34 Å)/(34 Å) films is close to that obtained in a pure Fe_3O_4 film and, therefore, has not been greatly altered even at 34-Å thickness by chemical or structural differences, or by reduction in dimensionality. However, the failure to see the Verwey transition from the insulator to conductor on warming shows that T_v , if it occurs, has been pushed above room temperature. Thus the Verwey transition has been changed in the modulated structure such that these materials appear to be in the low-temperature phase for all temperatures below 300 K. The change in T_v , without a change in the low-temperature conductivity is an unexpected result in the modulated structure which may be related to reduced dimensionality effects on this transition, but we have no further evidence on this conjecture. An obvious extension to resolve this question is to increase the period of the superlattice until the bulk conductivity is recovered, and this work is now in progress.

E. The effect of superlattice structure on perpendicular conductivity

A composite model again suggests that the conductivity for the perpendicular configuration samples should be twice that of the conductivity of NiO and independent of the superlattice wavelength. But it clearly fails to explain the perpendicular results since all of the perpendicular conductivity of the superlattices falls far above twice the value of the NiO. However, the electrical anisotropy for (34 Å)/(34 Å) and (68 Å)/(68 Å) samples are at the experimental limitation set by the length-to-area ratio. Thus these measured conductivities represent only an upper bound. We think, more importantly, that the conductivity of the (17 Å)/(17 Å) sample is not limited by the anisotropy as indicated above, but represents a new behavior associated with wavelengths < 34 Å.

V. CONCLUSIONS

X-ray and *in situ* RHEED results provide evidence that the $\text{Fe}_3\text{O}_4/\text{NiO}$ superlattice samples have been obtained with defined modulations. However, other physical properties, such as the conductivity and magnetization, cannot be automatically applied by a composite model. We have performed extensive conductivity studies on these samples and conclude that the pure thin films reasonably reproduce the bulk properties and, more important, that the superlattices indeed show modulated effects in the electric behavior. In addition, some interesting issues have been brought out in this study. (1) Although the Verwey transition was observed on the pure Fe_3O_4 films, the low dimensionality of the modulated structures seems to favor the low-temperature state. (2) The high-field dependence of the conductivity can be interpreted by the Poole-Frenkel effect in a wide temperature range for the pure materials. However, an anomalous behavior is observed around $T=40$ K for the superlattice samples with wavelengths less than 34 Å. (3) The low-field conductivity results also indicate a similar length scale in that the conductivity anisotropy is reduced when the modulated wavelength reaches below this value. (4) Finally, the conductivity measurements provide an important test of modulated properties. The great advantage of these studies is that the measurements can be done along both perpendicular and parallel directions. As a result, a single pair of (34 Å)/(34 Å) superlattice samples are sufficient to show the existence of a modulated property because of a substantial anisotropy for the current flow in two different directions.

We believe that quantitative results from both symmetry directions will be extremely important for understanding these materials and hope that such results stimulate theoretical work along these lines.

ACKNOWLEDGMENTS

We wish to thank C. M. Rey and W. G. Jenks for assistance in some resistivity measurements.

-
- ¹D. Adler, *Rev. Mod. Phys.* **40**, 714 (1968); *Solid State* **21**, 1 (1968).
²N. F. Mott, *Metal-Insulator Transition* (Taylor & Francis, London, 1990).
³J. M. Honig, in *The Metal and Nonmetallic States of Matter*, edited by P. P. Edwards and C. N. R. Rao (Taylor & Francis, London, 1985), p. 261.
⁴Y. Bando, S. Horii, and T. Takada, *Jpn. J. Appl. Phys.* **17**, 1037 (1978).
⁵T. Shigematsu, H. Ushigome, Y. Bando, and T. Takada, *J. Cryst. Growth* **50**, 801 (1980).
⁶T. Terashima and Y. Bando, *J. Appl. Phys.* **56**, 3445 (1984).
⁷T. Terashima and Y. Bando, *Thin Solid Films* **152**, 455 (1987).
⁸T. Koyano, Y. Kuroiwa, E. Kita, N. Saegusa, K. Ohshima, and A. Tasaki, *J. Appl. Phys.* **64**, 5764 (1988).
⁹T. Fujii, M. Takano, R. Katano, Y. Bando, and Y. Isouzumi, *J. Appl. Phys.* **66**, 3168 (1989).
¹⁰T. Fujii, M. Takano, R. Katano, Y. Bando, and Y. Isouzumi, *J. Appl. Phys.* **68**, 1735 (1990).
¹¹T. Fujii, M. Takano, R. Katano, Y. Bando, and Y. Isouzumi, *J. Cryst. Growth* **99**, 606 (1990).
¹²S. Yadavalli, M. H. Yang, and C. P. Flynn, *Phys. Rev. B* **41**, 7961 (1990).
¹³R. A. McKee, F. J. Walker, J. R. Conner, E. D. Specht, and D. E. Zelmon, *Appl. Phys. Lett.* **59**, 782 (1991).
¹⁴D. M. Lind, S. D. Berry, G. Chern, H. Mathias, and L. R. Testardi, *Phys. Rev. B* **45**, 1838 (1992).
¹⁵S. D. Berry, D. M. Lind, G. Chern, H. Mathias, and L. R. Testardi (unpublished).
¹⁶B. H. Brandow, *Adv. Phys.* **26**, 651 (1977).
¹⁷International Conference on the Metal-Nonmetal Transition [*Rev. Mod. Phys.* **40**, 673 (1968)].
¹⁸G. Chern, S. D. Berry, D. M. Lind, H. Mathias, and L. R. Testardi, *Appl. Phys. Lett.* **58**, 2512 (1991).
¹⁹Harald Bottger and Dieter Wegener, in *Hopping and Related Phenomena*, edited by Hellmut Fritzsche and Michael Pollak

(World Scientific, Singapore, 1990).

²⁰N. F. Mott, *Philos. Mag.* **24**, 911 (1971).

²¹C. J. Adkins, S. M. Freake, and E. M. Hamilton, *Philos. Mag.* **22**, 183 (1970).

²²We should also point out that Mott has given a more careful examination of Eq. (1) and suggested that there is a difference between the intrinsic and the extrinsic semiconductors. Equation (1) is suitable for the intrinsic ones but the β_i needs

to be multiplied by 2 for the compensated extrinsic case and this would lead to dielectric constants of 40.5 and 16.6 for the Fe₃O₄ and the NiO, respectively.

²³P. A. Miles, W. B. Westphal, and A. von Hippel, *Rev. Mod. Phys.* **29**, 279 (1957).

²⁴E. U. Condon and H. Odishaw, *Handbook of Physics*, 1st ed. (McGraw-Hill, New York, 1958).